ARCHIVES OF MECHANICS
Arch. Mech. **73** (1), 67–81, 2021, DOI: 10.24423/aom.3639

Uniform stress field inside a non-parabolic open inhomogeneity interacting with a mode III crack

X. WANG[1)], P. SCHIAVONE[2)]

[1)] *School of Mechanical and Power Engineering, East China University of Science and Technology, 130 Meilong Road, Shanghai 200237, China, e-mail: xuwang@ecust.edu.cn*

[2)] *Department of Mechanical Engineering, University of Alberta, 10-203 Donadeo Innovation Centre for Engineering Edmonton, Alberta Canada T6G 1H9, e-mail: p.schiavone@ualberta.ca*

Using conformal mapping techniques, analytic continuation and the theory of Cauchy singular integral equations, we prove that a non-parabolic open inhomogeneity embedded in an elastic matrix subjected to a uniform remote anti-plane stress nevertheless admits an internal uniform stress field despite the presence of a finite mode III crack in its vicinity. Our analysis indicates that: (i) the internal uniform stress field is independent of the specific shape of the inhomogeneity and the presence of the finite crack; (ii) the existence of the finite crack plays a key role in the non-parabolic open shape of the inhomogeneity and in the non-uniform stresses in the surrounding matrix; (iii) the two-term asymptotic expansion at infinity of the stress field in the matrix is independent of the presence of the finite crack. Detailed numerical results are presented to demonstrate the proposed theory.

Key words: non-parabolic inhomogeneity, mode III crack, uniform stress field, anti-plane elasticity, conformal mapping, singular integral equation.

1. Introduction

In the design and manufacture of composite materials, inhomogeneities (material regions with distinct elastic properties) are often introduced into a host elastic material (known as the 'matrix') for the purpose of improving the mechanical properties of the composite (e.g. strength, durability, resistance to fatigue or corrosion etc.). The ability to design inhomogeneities (via shape and elastic properties), which enclose a uniform stress distribution, is of particular interest. This situation is often regarded as optimal since it eliminates the possibility of stress peaks within the inhomogeneity which are known to be responsible for the failure of the entire composite. Consequently, much attention has been devoted in the literature to the design of inhomogeneities which enclose uniform stress distributions.

In a seminal contribution, Eshelby [1] conjectured that ellipses and ellipsoids are the only shape of elastic inhomogeneities permitting internal uniform stresses and strains when the surrounding matrix is subjected to a uniform applied field. Subsequent analyses of Eshelby's conjecture have been conducted by various authors (see, for example, [2–12]). A comprehensive review can be found in Zhou *et al.* [13]. The objective, as always, is to identify conditions under which the stress distribution inside embedded inhomogeneities remains uniform. In some cases, this design requirement is to be established in the presence of other constituents introduced into the composite either intentionally (to induce specific properties) or unintentionally via the manufacturing process. To this end, it has recently been demonstrated by Wang *et al.* [14] that when a finite mode III crack is present in the vicinity of a non-elliptical elastic inhomogeneity bounded by a closed curvilinear contour or interface, the stresses inside the inhomogeneity may nevertheless remain uniform through a judicious design of the non-elliptical shape of the inhomogeneity and the location of the finite crack. The non-elliptical closed shape of the inhomogeneity permitting internal uniform stresses is attributed solely to the presence of the nearby finite mode III crack. Very recently, Wang and Schiavone [15] have established the remarkable and surprising result in both anti-plane and in-plane elasticity that the internal stresses inside a parabolic inhomogeneity with an open interface are unconditionally uniform when the surrounding matrix is subjected to uniform remote stresses. It is natural then to pose the following question: if a finite crack is located near a non-parabolic elastic inhomogeneity with an open interface, can the internal stress field inside the inhomogeneity be maintained uniform via a proper design of the non-parabolic shape of the inhomogeneity together with the location of the finite crack? This study endeavors to answer this question. We anticipate that the two major difficulties arising from the analysis concern the non-parabolic open shape of the inhomogeneity and the presence of the finite crack in the matrix. Potential applications of our findings arise, for example, in the design of capillary barriers [16, 17].

With the above objective in mind, we employ conformal mapping techniques, together with analytic continuation [18, 19] and the theory of Cauchy singular integral equations [20] to prove that when a finite mode III crack is present in the neighborhood of a non-parabolic open inhomogeneity, the stress field inside the inhomogeneity can indeed remain uniform when the matrix is subjected to uniform remote anti-plane shear stress. The real density function appearing in the conformal mapping function can be determined through the solution of a Cauchy singular integral equation obtained by imposing the traction-free condition on the crack faces. The singular integral equation is solved numerically using the Gauss-Chebyshev integration formula [21] which is also used quite conveniently to evaluate the finite integral embedded in the mapping function and the non-uniform stress field in the matrix. We derive the displacement jump across the crack faces and the stress intensity factors at the two crack tips. Our analysis indicates that: (i) the internal uniform stress field inside the inhomogeneity is independent of the specific shape of the inhomogeneity and the presence of the nearby finite crack; (ii) the existence of the finite crack exerts a significant influence on the non-parabolic open shape of the inhomogeneity and on the non-uniform stress field in the surrounding matrix; (iii) the two-term asymptotic expansion at infinity of the stress field in the matrix is also independent of the existence of the finite crack. Detailed numerical results illustrating the non-parabolic shapes of the inhomogeneity together with the accompanying locations of the finite crack and the stress distributions in the two-phase composite are presented to validate the feasibility of the proposed theory.

2. Complex variable formulation

We first establish a Cartesian coordinate system $\{x_i\}$ $(i = 1, 2, 3)$. Under anti-plane shear deformations of an isotropic elastic material, the two anti-plane shear stress components σ_{31} and σ_{32}, the out-of-plane displacement $w = u_3$ and the stress function ϕ can be expressed in terms of a single analytic function $f(z)$ of the complex variable $z = x_1 + \mathrm{i}x_2$ as [22]

$$\sigma_{32} + \mathrm{i}\sigma_{31} = \mu f'(z), \qquad \phi + \mathrm{i}\mu w = \mu f(z), \tag{2.1}$$

where μ is the shear modulus, and the two anti-plane stress components can be expressed in terms of the stress function as [22]

$$\sigma_{32} = \phi_{,1}, \qquad \sigma_{31} = -\phi_{,2}. \tag{2.2}$$

3. Uniformity of stresses inside the inhomogeneity

As shown in Fig. 1, we consider a domain in $\mathbb{R}^2$, infinite in extent, containing a non-parabolic open elastic inhomogeneity with elastic properties distinct from those of the surrounding matrix. In addition, the matrix is weakened by a traction-free finite mode III crack $\{a \leq x_1 \leq b,\, x_2 = 0^{\pm}\}$. Let S_1 and S_2 denote the inhomogeneity and the matrix, respectively, both of which are perfectly bonded through the interface L. The crack is denoted by C. In addition, the matrix is subjected to uniform remote anti-plane shear stresses $(\sigma_{31}^{\infty}, \sigma_{32}^{\infty})$. Throughout the paper, the subscripts 1 and 2 are used to identify the respective quantities in S_1 and S_2.

The corresponding boundary value problem takes the following form:

$$\begin{aligned} f_2(z) + \overline{f_2(z)} &= \Gamma f_1(z) + \Gamma\overline{f_1(z)}, \\ f_2(z) - \overline{f_2(z)} &= f_1(z) - \overline{f_1(z)}, \quad z \in L; \end{aligned} \tag{3.1a}$$

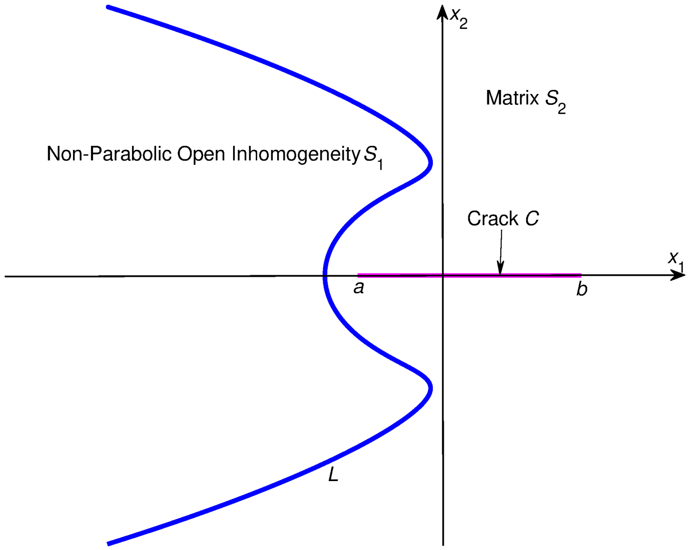

FIG. 1. A model III crack interacting with a non-parabolic open inhomogeneity with internal uniform stersses when the matrix is subjected to uniform remote anti-plane sterss.

(3.1b) $$f_2'^{+}(z) + \overline{f_2'^{+}(z)} = f_2'^{-}(z) + \overline{f_2'^{-}(z)} = 0, \qquad z \in C;$$

(3.1c) $$f_2(z) \cong \frac{\sigma_{32}^\infty + \mathrm{i}\sigma_{31}^\infty}{\mu_2} z + O(z^{1/2}), \qquad |z| \to \infty,$$

where $\Gamma = \mu_1/\mu_2$. Equation (3.1a) describes the continuity of traction and displacement across the perfectly bonded interface; Eq. (3.1b) describes the traction-free condition on the crack faces; Eq. (3.1c) characterizes the asymptotic behavior of $f_2(z)$ at infinity due to the remote anti-plane loading.

We introduce the following conformal mapping function for the matrix region

(3.2) $$z = \omega(\xi) = \xi^2 + H^{1/2} \int_{\xi_1}^{\xi_2} q(\eta) \ln(\xi + \eta - 2H^{1/2})\, d\eta,$$
$$\xi = \omega^{-1}(z),\ H > 0,\ \xi_2 > \xi_1 > H^{1/2},\ \mathrm{Re}\{\xi\} \geq H^{1/2},$$

where $q(\eta)$ is an unknown dimensionless real density function to be determined, the parameter H has the dimension of length, $\xi_1 = \omega^{-1}(a)$ and $\xi_2 = \omega^{-1}(b)$ or conversely $a = \omega(\xi_1)$ and $b = \omega(\xi_2)$. As it is shown in Fig. 2, using the mapping function in Eq. (3.2), the exterior of the inhomogeneity is mapped onto the right half-plane $\mathrm{Re}\{\xi\} \geq H^{1/2}$ in the ξ-plane; the inhomogeneity-matrix interface L is mapped onto the vertical straight line: $\mathrm{Re}\{\xi\} = H^{1/2}$,

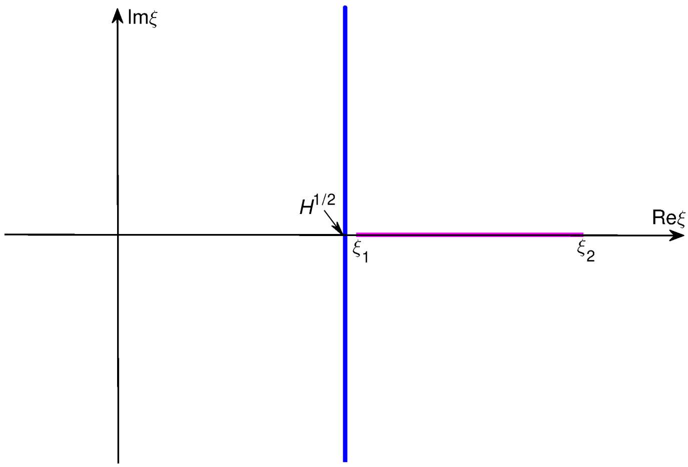

Fig. 2. The problem in the ξ-plane.

$-\infty < \mathrm{Im}\{\xi\} < +\infty$ in the ξ-plane; the finite crack is mapped onto the slit $\{\xi_1 \le \mathrm{Re}\{\xi\} \le \xi_2, \mathrm{Im}\{\xi\} = 0^{\pm}\}$ in the ξ-plane. The interface L will become a parabola described by L: $x_1 = H - x_2^2/4H$ when $q(\eta) = 0$ or when the crack is far from the inhomogeneity.

Now suppose that the internal stress field inside the non-parabolic inhomogeneity is uniform, characterized by

$$f_1(z) = Az, \qquad z \in S_1, \tag{3.3}$$

where A is a complex constant to be determined.

By imposing the continuity conditions of traction and displacement across the interface in Eq. (3.1a) with the use of Eq. (3.3) and with the aid of analytic continuation [18, 19], we arrive at

$$f_2(\xi) = f_2(\omega(\xi)) = \frac{\Gamma+1}{2} A\omega(\xi) + \frac{\Gamma-1}{2} \bar{A}\bar{\omega}(2H^{1/2} - \xi), \qquad \mathrm{Re}\{\xi\} \ge H^{1/2}, \tag{3.4}$$

which can be more explicitly written in the form

$$\begin{aligned} f_2(\xi) = {} & \frac{A(\Gamma+1) + \bar{A}(\Gamma-1)}{2}\xi^2 - 2H^{1/2}\bar{A}(\Gamma-1)\xi \\ & + \frac{H^{1/2}\bar{A}(\Gamma-1)}{2} \int_{\xi_1}^{\xi_2} q(\eta) \ln(\eta - \xi)\, d\eta \\ & + \frac{H^{1/2}A(\Gamma+1)}{2} \int_{\xi_1}^{\xi_2} q(\eta) \ln(\xi + \eta - 2H^{1/2})\, d\eta, \qquad \mathrm{Re}\{\xi\} \ge H^{1/2}. \end{aligned} \tag{3.5}$$

Using Eq. (3.4) to satisfy the remote asymptotic behavior in Eq. (3.1c), we arrive at the following relationship

$$\frac{A(\Gamma+1)+\bar{A}(\Gamma-1)}{2}=\frac{\sigma_{32}^{\infty}+\mathrm{i}\sigma_{31}^{\infty}}{\mu_2}. \tag{3.6}$$

In order to ensure the single-valuedness of the displacement and balance of force for any contour in the matrix surrounding the crack C, following an inspection of Eq. (3.5), the following constraint should be satisfied

$$\int_{\xi_1}^{\xi_2} q(\eta)\,d\eta=0. \tag{3.7}$$

In addition, we arrive at a Cauchy singular integral equation by assuming that the constant A is real valued and by imposing the traction-free condition on the crack faces in Eq. (3.1b) as follows

$$\int_{\xi_1}^{\xi_2}\frac{q(\eta)}{\xi-\eta}\,d\eta+\frac{1}{K}\int_{\xi_1}^{\xi_2}\frac{q(\eta)}{\xi+\eta-2H^{1/2}}\,d\eta=4-\frac{2(K+1)}{K}H^{-1/2}\xi,\ \ \xi_1<\xi<\xi_2, \tag{3.8}$$

where K is a mismatch parameter defined by

$$K=\frac{\Gamma-1}{\Gamma+1},\qquad -1<K<1. \tag{3.9}$$

Using the following standard change of variables

$$x=\frac{2\xi-\xi_1-\xi_2}{\xi_2-\xi_1},\qquad t=\frac{2\eta-\xi_1-\xi_2}{\xi_2-\xi_1}, \tag{3.10}$$

Eqs. (3.7) and (3.8) can be recast into the following normalized form

$$\begin{aligned}&\int_{-1}^{1}\frac{q(t)}{t-x}\,dt+\frac{\xi_1-\xi_2}{K}\int_{-1}^{1}\frac{q(t)}{(t+x)(\xi_2-\xi_1)+2(\xi_1+\xi_2)-4H^{1/2}}\,dt\\ &\qquad=\frac{K+1}{K}H^{-1/2}[x(\xi_2-\xi_1)+\xi_1+\xi_2]-4,\qquad -1<x<1,\\ &\int_{-1}^{1}q(t)\,dt=0,\end{aligned} \tag{3.11}$$

where $q(t)=q(\eta)$.

The unknown real density function $q(t)$ can be written as

$$q(t) = \frac{Q(t)}{\sqrt{1-t^2}}, \qquad -1 \le t \le 1, \tag{3.12}$$

where $Q(t)$ is an unknown bounded function in $[-1, 1]$.

Substituting Eq. (3.12) into Eq. (3.11) and using the Gauss–Chebyshev integration formula [21], the singular integral equation in Eq. (13) reduces to the following set of linear algebraic equations for the n unknowns $Q(t_1), Q(t_2), \ldots, Q(t_n)$

$$\begin{aligned} &\sum_{k=1}^{n} \frac{1}{n} Q(t_k) \left[\frac{1}{t_k - x_r} + \frac{\xi_1 - \xi_2}{K[(t_k + x_r)(\xi_2 - \xi_1) + 2(\xi_1 + \xi_2) - 4H^{1/2}]} \right] \\ &\qquad = \frac{1}{\pi} \left\{ \frac{K+1}{K} H^{-1/2} [x_r(\xi_2 - \xi_1) + \xi_1 + \xi_2] - 4 \right\}, \\ &\sum_{k=1}^{n} \frac{1}{n} Q(t_k) = 0, \quad t_k = \cos\frac{\pi}{2n}(2k-1),\ x_r = \cos\frac{\pi r}{n},\ r = 1, 2, \ldots, n-1, \end{aligned} \tag{3.13}$$

from which all of the n unknowns can be uniquely determined.

Also, by using the Gauss–Chebyshev integration formula, the mapping function in Eq. (3.2) containing a finite integral can be approximated as

$$\begin{aligned} z &= \omega(\xi) \\ &= \xi^2 + \frac{H^{1/2}(\xi_2 - \xi_1)}{2} \int_{-1}^{1} q(t) \ln\left[\xi + \frac{1}{2} t(\xi_2 - \xi_1) + \frac{1}{2}(\xi_1 + \xi_2) - 2H^{1/2}\right] dt \\ &\approx \xi^2 + \frac{\pi}{2} H^{1/2}(\xi_2 - \xi_1) \sum_{k=1}^{n} \frac{1}{n} Q(t_k) \\ &\quad \times \ln\left[\xi + \frac{1}{2} t_k(\xi_2 - \xi_1) + \frac{1}{2}(\xi_1 + \xi_2) - 2H^{1/2}\right], \end{aligned} \tag{3.14}$$

where t_k has been defined in Eq. (3.13).

Once A is taken to be real, it is simply deduced from Eq. (3.6) that

$$A = \frac{\sigma_{32}^{\infty}}{\mu_1}, \qquad \sigma_{31}^{\infty} = 0. \tag{3.15}$$

Thus, the internal uniform stress field inside the non-parabolic inhomogeneity is given simply by

$$\sigma_{32} = \sigma_{32}^{\infty}, \qquad \sigma_{31} = 0, \qquad z \in S_1. \tag{3.16}$$

By substituting Eq. (3.5) into Eq. (2.1), the stresses are non-uniformly distributed in the matrix as follows

$$\sigma_{32}+\mathrm{i}\sigma_{31} = \sigma_{32}^{\infty} - \frac{\sigma_{32}^{\infty}K\left[4+\int_{\xi_1}^{\xi_2}\frac{q(\eta)}{\eta-\xi}\,d\eta+\int_{\xi_1}^{\xi_2}\frac{q(\eta)}{\xi+\eta-2H^{1/2}}\,d\eta\right]}{(K+1)\left[2H^{-1/2}\xi+\int_{\xi_1}^{\xi_2}\frac{q(\eta)}{\xi+\eta-2H^{1/2}}\,d\eta\right]}, \qquad \mathrm{Re}\{\xi\}\geq H^{1/2}. \tag{3.17}$$

The remote asymptotic behavior of the stresses can be obtained from Eq. (3.17) as:

$$\sigma_{32}+\mathrm{i}\sigma_{31}\cong\sigma_{32}^{\infty}-\frac{2\sigma_{32}^{\infty}K}{K+1}\sqrt{\frac{H}{z}}+O\left(\frac{1}{z}\right), \qquad |z|\to\infty. \tag{3.18}$$

We can see from Eqs. (3.16) and (3.17) that $\sigma_{31}=0$ along the x_1-axis outside the crack. By using the Plemelj formulas [20, 23], the stress component σ_{31} on the upper and lower crack faces can be obtained from Eq. (3.17) as follows:

$$\sigma_{31}^{+}(x_1)=-\sigma_{31}^{-}(x_1) = -\frac{\pi K\sigma_{32}^{\infty}q(\xi)}{(K+1)\left[2H^{-1/2}\xi+\int_{\xi_1}^{\xi_2}\frac{q(\eta)}{\xi+\eta-2H^{1/2}}d\eta\right]}, \qquad \xi_1<\xi<\xi_2. \tag{3.19}$$

It is not difficult to verify that by using Eqs. (3.7) and (3.19)

$$\int_a^b\sigma_{31}^{+}(x_1)\,dx_1=\int_a^b\sigma_{31}^{-}(x_1)\,dx_1=0. \tag{3.20}$$

The displacement jump across the crack faces can also be derived from Eq. (3.19) as

$$\Delta w=w^{+}-w^{-}=-\frac{2\pi K\sigma_{32}^{\infty}H^{1/2}}{\mu_2(K+1)}\int_{\xi_1}^{\xi}q(\eta)\,d\eta, \qquad \xi_1<\xi<\xi_2. \tag{3.21}$$

It is clear that the stresses exhibit the square root singularity at the two crack tips $z=a$ and $z=b$ [20]. Furthermore, the mode III stress intensity factors at the two crack tips can be extracted from the displacement jump across the crack faces in Eq. (3.21) as follows

$$\begin{aligned} K_{\mathrm{III}}(a)&=-\frac{\pi K\sigma_{32}^{\infty}H^{1/2}Q(-1)}{K+1}\sqrt{\frac{\pi(\xi_2-\xi_1)}{2\omega'(\xi_1)}},\\ K_{\mathrm{III}}(b)&=\frac{\pi K\sigma_{32}^{\infty}H^{1/2}Q(1)}{K+1}\sqrt{\frac{\pi(\xi_2-\xi_1)}{2\omega'(\xi_2)}}. \end{aligned} \tag{3.22}$$

It is seen from the above analysis that: (i) the internal uniform stress field in Eq. (3.16) is independent of the specific shape of the inhomogeneity and the presence of the nearby finite mode III crack; (ii) the existence of the finite crack exerts a significant influence on the non-parabolic shape of the inhomogeneity and on the non-uniform stress distribution in the matrix through the real density function $q(\eta)$ and the two real parameters ξ_1 and ξ_2; (iii) the two-term asymptotic expansion at infinity of the stress field in the matrix in Eq. (3.18) is independent of the presence of the finite crack. The stresses in the matrix outside the crack in Eq. (3.17), $\sigma_{31}^{\pm}$ in Eq. (3.19) on the two crack faces, and the two stress intensity factors in Eq. (3.22) can also be conveniently evaluated by using the Gauss–Chebyshev integration formula.

4. Numerical results

In this section, numerical results for the non-parabolic shapes of the inhomogeneity and the stress distributions in the composite are presented to demonstrate the theory proposed in Section 3. In fact, the configuration in Fig. 1 is obtained by choosing the following parameters

$$K = -0.5, \qquad \xi_1 = 1.05H^{1/2}, \qquad \xi_2 = 2.05H^{1/2}. \tag{4.1}$$

In this case, the inhomogeneity is softer than the matrix ($\Gamma = 1/3 < 1$). The non-parabolic shape of the inhomogeneity and the location of the finite

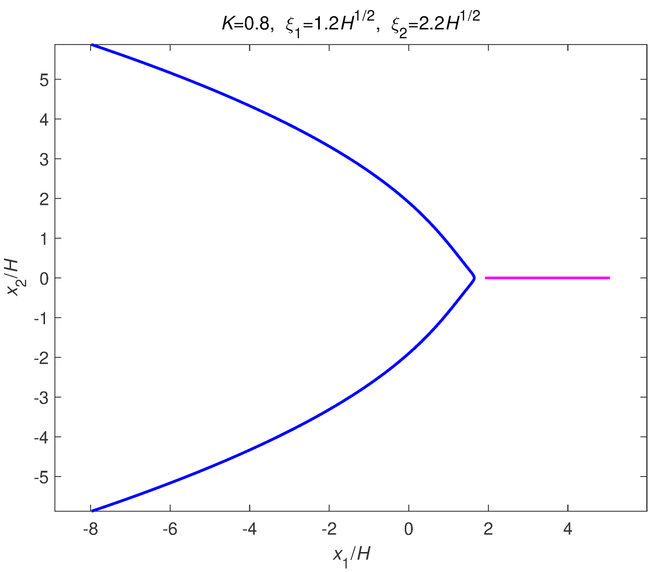

FIG. 3. The non-parabolic shape of the inhomogeneity and the location of the finite crack when choosing $K = 0.8$, $\xi_1 = 1.2H^{1/2}$, $\xi_2 = 2.2H^{1/2}$.

crack when choosing $K = 0.8$, $\xi_1 = 1.2H^{1/2}$, $\xi_2 = 2.2H^{1/2}$ are illustrated in Fig. 3 in which case the inhomogeneity is harder than the matrix ($\Gamma = 9 > 1$). A comparison of Fig. 1 with Fig. 3 reveals that the non-parabolic shape for

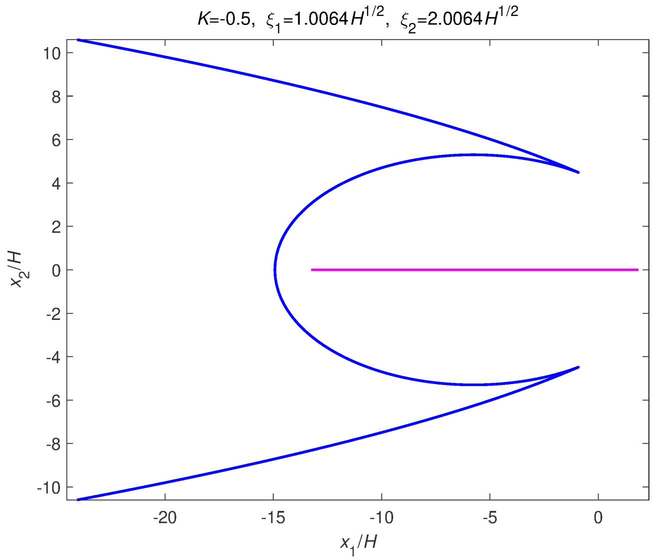

FIG. 4. The non-parabolic shape of the inhomogeneity and the location of the finite crack when choosing $K = -0.5$, $\xi_1 = 1.0064H^{1/2}$, $\xi_2 = 2.0064H^{1/2}$.

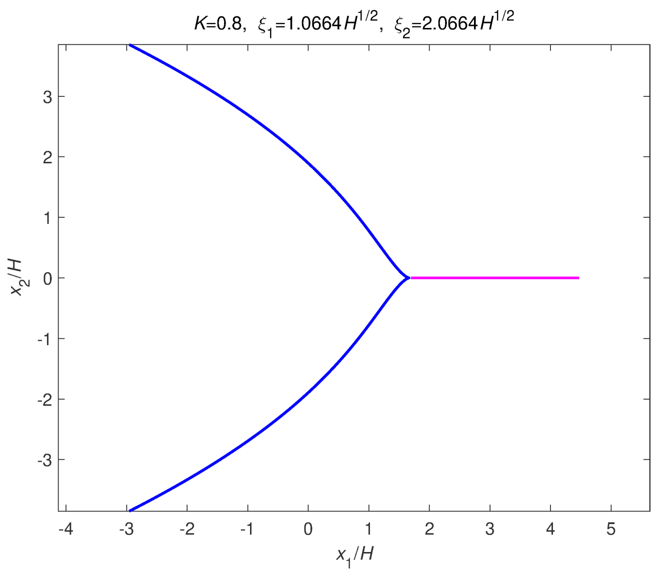

FIG. 5. The non-parabolic shape of the inhomogeneity and the location of the finite crack when choosing $K = 0.8$, $\xi_1 = 1.0064H^{1/2}$, $\xi_2 = 2.0064H^{1/2}$.

a soft inhomogeneity ($\Gamma < 1$) permitting internal uniform stresses is quite different than that for a hard inhomogeneity ($\Gamma > 1$) permitting internal uniform stresses.

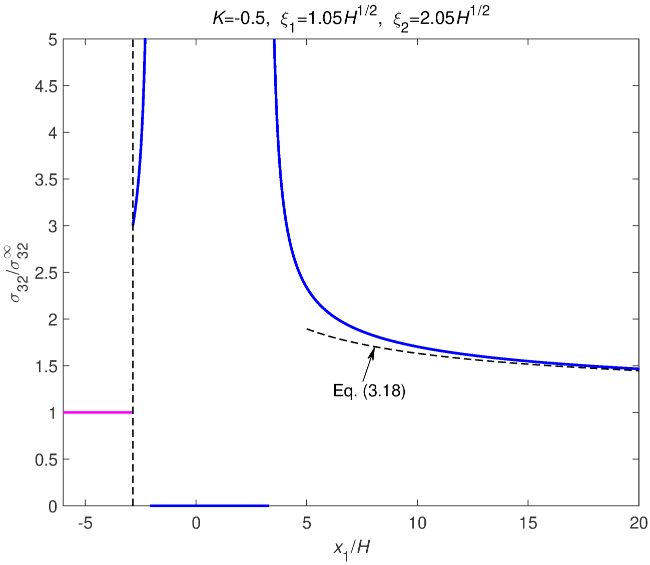

FIG. 6. The distribution od σ_{32} along the x_1-axis when choosing $K = -0.5$, $\xi_1 = 1.05H^{1/2}$, $\xi_2 = 2.05H^{1/2}$.

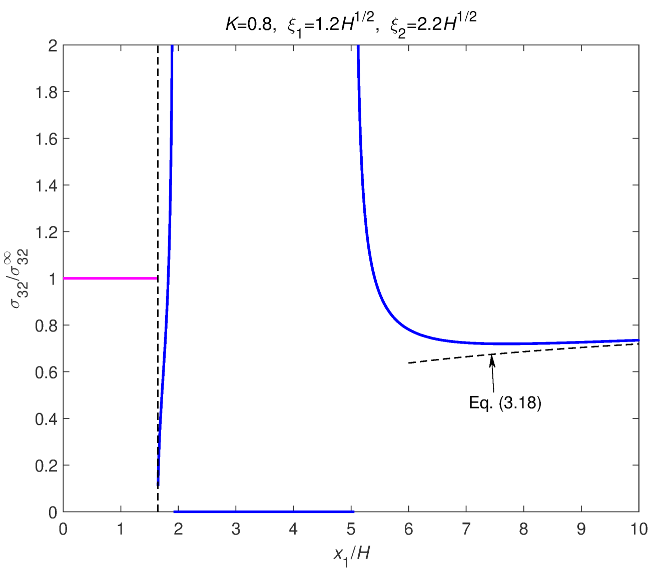

FIG. 7. The distribution od σ_{32} along the x_1-axis when choosing $K = 0.8$, $\xi_1 = 1.2H^{1/2}$, $\xi_2 = 2.2H^{1/2}$.

Our results indicate that it is permissible for the interface L to have two sharp corners for a soft inhomogeneity (Fig. 4) and only one sharp corner for a hard inhomogeneity (Fig. 5). At these sharp corners, we have $\omega'(\xi) = 0$. However,

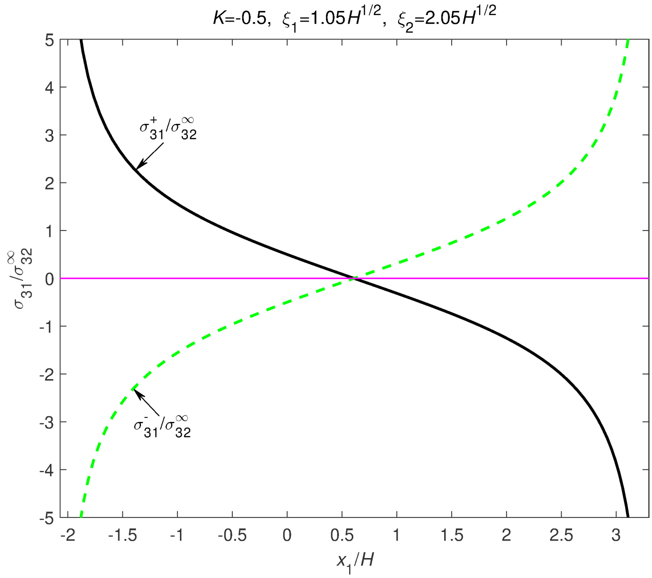

FIG. 8. The distribution od σ_{31} on the upper and lower crack faces when choosing $K = -0.5$, $\xi_1 = 1.05H^{1/2}$, $\xi_2 = 2.05H^{1/2}$.

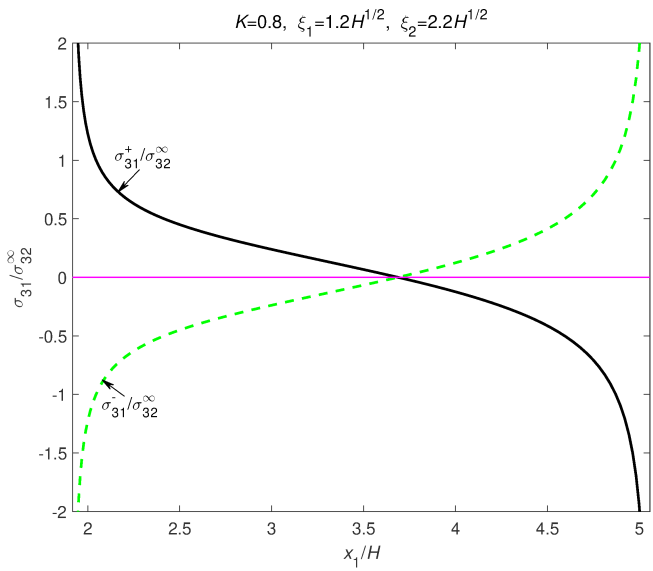

FIG. 9. The distribution od σ_{31} on the upper and lower crack faces when choosing $K = 0.8$, $\xi_1 = 1.2H^{1/2}$, $\xi_2 = 2.2H^{1/2}$.

following an examination of Eqs. (2.1) and (3.4), we find that the stresses in the matrix remain bounded at these sharp corners on the interface.

We illustrate in Figs. 6 and 7 the distribution of σ_{32} along the x_1-axis. In Fig. 6, $\sigma_{32} = 3\sigma_{32}^{\infty} = \sigma_{32}^{\infty}/\Gamma$ at the interface on the matrix side. In Fig. 7, $\sigma_{32} = 0.1111\sigma_{32}^{\infty} = \sigma_{32}^{\infty}/\Gamma$ at the interface on the matrix side. These observations reflect the fact that the continuity of displacement (or equivalently the continuity of the tangential derivative of the displacement) along the perfectly bonded inhomogeneity-matrix interface has been satisfied. As $x_1 \to +\infty$, σ_{32} in the matrix in both Figs. 6 and 7 behave in a manner according to Eq. (3.18). It is also apparent from Figs. 6 and 7 that the stress field is singular at the two crack tips. The stress intensity factors at the two crack tips can be determined from Eq. (3.22) as follows

$$\text{(4.2)} \qquad \frac{K_{\text{III}}(a)}{\sigma_{32}^{\infty} H^{1/2}} = 5.7001, \qquad \frac{K_{\text{III}}(b)}{\sigma_{32}^{\infty} H^{1/2}} = 5.7142$$
$$\text{when } K = -0.5,\ \xi_1 = 1.05H^{1/2},\ \xi_2 = 2.05H^{1/2};$$

$$\text{(4.3)} \qquad \frac{K_{\text{III}}(a)}{\sigma_{32}^{\infty} H^{1/2}} = 0.8444, \qquad \frac{K_{\text{III}}(b)}{\sigma_{32}^{\infty} H^{1/2}} = 1.2267$$
$$\text{when } K = 0.8,\ \xi_1 = 1.2H^{1/2},\ \xi_2 = 2.2H^{1/2},$$

the correctness of which has been verified from the results in Figs. 6 and 7. We see from Eqs. (4.2) and (4.3) that: (i) the magnitudes of the stress intensity factors at the two crack tips in the presence of a soft inhomogeneity with $K = -0.5$ is larger than those of $K_{\text{III}}(a) = K_{\text{III}}(b) = \sigma_{32}^{\infty}\sqrt{\frac{\pi}{2}(b-a)} = 2.9043\sigma_{32}^{\infty}H^{1/2}$ for the same crack in an infinite homogeneous medium; (ii) the magnitudes of the stress intensity factors at the two crack tips in the presence of a hard inhomogeneity with $K = 0.8$ is lower than those of $K_{\text{III}}(a) = K_{\text{III}}(b) = \sigma_{32}^{\infty}\sqrt{\frac{\pi}{2}(b-a)} = 2.2211\sigma_{32}^{\infty}H^{1/2}$ for the same crack in an infinite homogeneous medium.

Finally, we illustrate in Figs. 8 and 9 the distribution of σ_{31} on the upper and lower crack faces. It is clear from Figs. 8 and 9 that σ_{31} is singular at the two crack tips and that the conditions in Eq. (3.20) are satisfied.

5. Conclusions

We have proved that within the framework of anti-plane elasticity, the internal stresses inside a non-parabolic open inhomogeneity in the vicinity of a finite mode III crack lying on the x_1-axis in the matrix can nevertheless be maintained uniform when the matrix is subjected only to a uniform remote anti-plane stress σ_{32}^{∞} with $\sigma_{31}^{\infty} = 0$. The conformal mapping function is introduced in Eq. (2.2) with the real density function $q(\eta)$ determined through numerical solution via the application of the Gauss–Chebyshev integration formula to the Cauchy singular integral equation in Eq. (3.8) together with the constraint in Eq. (3.7). The internal uniform stress field inside the inhomogeneity is given by Eq. (3.16), the non-uniform stress field in the matrix is given by Eq. (3.17) with its two-term asymptotic expansion at infinity given by Eq. (3.18). The displacement jump across the crack faces and the stress intensity factors at the two crack tips are given by Eqs. (3.21) and (3.22), respectively.

Our method extends to the problem of an anticrack (or rigid line inclusion) interacting with a non-parabolic inhomogeneity with internal uniform stresses. In this case, the matrix should be subjected to the uniform remote anti-plane stress σ_{31}^{∞} with $\sigma_{32}^{\infty} = 0$ and the uniform stresses inside the non-parabolic inhomogeneity are simply given by: $\sigma_{31} = \Gamma\sigma_{31}^{\infty}$, $\sigma_{32} = 0$. The problem of a Zener–Stroh crack with a net screw dislocation Burgers vector near a non-parabolic inhomogeneity permitting internal uniform stresses can also be addressed quite conveniently using this method.

Acknowledgements

This work is supported by the National Natural Science Foundation of China (the Grant No. 11272121) and through a Discovery Grant from the Natural Sciences and Engineering Research Council of Canada (the Grant No: RGPIN – 2017 - 03716115112).

References

1. J.D. Eshelby, *Elastic inclusions and inhomogeneities*, Progress in Solid Mechanics, vol. II, 89–140, 1961.
2. G.P Sendeckyj, *Elastic inclusion problem in plane elastostatics*, International Journal of Solids and Structures, **6**, 1535–1543, 1970.
3. C.Q. Ru, P. Schiavone, *On the elliptic inclusion in anti-plane shear*, Mathematics and Mechanics of Solids, **1**, 327–333, 1996.
4. V.A. Lubarda, X. Markenscoff, *On the absence of Eshelby property for non-ellipsoidal inclusions*, International Journal of Solids and Structures, **35**, 3405–3411, 1998.
5. X. Markenscoff, *Inclusions with constant eigenstress*, Journal of the Mechanics and Physics of Solids, **46**, 2297–2301, 1998.
6. X. Markenscoff, *On the shape of the Eshelby inclusion*, Journal of Elasticity, **49**, 163–166, 1998.
7. Y.A. Antipov, P. Schiavone, *On the uniformity of stresses inside an inhomogeneity of arbitrary shape*, IMA Journal of Applied Mathematics, **68**, 299–311, 2003.

8. L.P. Liu, *Solution to the Eshelby conjectures*, Proceedings of the Royal Society of London A, **464**, 573–594, 2008.
9. H. Kang, E. Kim, G.W. Milton, *Inclusion pairs satisfying Eshelby's uniformity property*, SIAM Journal of Applied Mathematics, **69**, 577–595, 2008.
10. H. Kang, G.W. Milton, *Solutions to the Pólya–Szegö conjecture and the weak Eshelby conjecture*, Archive for Rational Mechanics and Analysis, **188**, 93–116, 2008.
11. H. Ammari, Y. Capdeboscq, H. Kang, H. Lee, G.W. Milton, H. Zribi, *Progress on the strong Eshelby's conjecture and extremal structures for the elastic moment tensor*, Journal de Mathématiques Pures et Appliquées, **94**, 93–106, 2010.
12. X. Wang, *Uniform fields inside two non-elliptical inclusions*, Mathematics and Mechanics of Solids, **17**, 736–761, 2012.
13. K. Zhou, H.J. Hoh, X. Wang, L.M. Keer, J.H.L. Pang, B. Song, Q.J. Wang, *A review of recent works on inclusions*, Mechanics of Materials, **60**, 144–158, 2013.
14. X. Wang, L. Chen, P. Schiavone, *Uniformity of stresses inside a non-elliptical inhomogeneity interacting with a mode III crack*, Proceedings of the Royal Society of London A, **474,** 2218, 20180304, 2018.
15. X. Wang, P. Schiavone, *Uniformity of stresses inside a parabolic inhomogeneity*, Journal of Applied Mathematics and Physics, **71**, 2, 48, 2020.
16. J.R. Philip, *Seepage shedding by parabolic capillary barriers and cavities*, Water Resources Research, **34**, 2827–2835, 1998.
17. A.R. Kacimov, Yu.V. Obnosov, *Steady water flow around parabolic cavities and through parabolic inclusions in unsaturated and saturated soils*, Journal of Hydrology, **238**, 65–77, 2000.
18. Z.G. Suo, *Singularities interacting with interfaces and cracks*, International Journal of Solids and Structures, **25**, 1133–1142, 1989.
19. C.Q. Ru, *Analytic solution for Eshelby's problem of an inclusion of arbitrary shape in a plane or half-plane*, ASME Journal of Applied Mechanics, **66**, 315–322, 1999.
20. N.I. Muskhelishvili, *Singular Integral Equations*, P. Noordhoff Ltd., Groningen, Holland, 1953.
21. F. Erdogan, G.D. Gupta, *On the numerical solution of singular integral equations*, Quarterly of Applied Mathematics, **29**, 525–534, 1972.
22. T.C.T. Ting, *Anisotropic Elasticity-Theory and Applications*, Oxford University Press, New York, 1996.
23. Z.G. Suo, *Complex Variable Method*, [in:] *Advanced Elasticity*, *Lecture Notes*, Harvard University, 2007.

Received August 19, 2020; revised version November 24, 2020.
Published online January 21, 2021.